Gating individual nanotubes and crosses with scanning probes

Thomas W. Tombler, Chongwu Zhou, Jing Kong, and Hongjie Dai[a)]
Department of Chemistry, Stanford University, Stanford, California 94305

(Received 3 November 1999; accepted for publication 1 February 2000)

Atomic force microscopy tips are used to apply point-like local gates to manipulate the electrical properties of individual single-walled carbon nanotubes (SWNT) contacted by Ti electrodes. Depleting a semiconducting SWNT at a local point along its length leads to orders of magnitude decrease of the nanotube conductance, whereas local gating to metallic SWNTs causes no change in the conductance of the system. These results shed light into gating effects on metal-tube contacts. Electrical properties of SWNT crosses are also investigated. Scanning-probe gating is used to identify the metallic or semiconducting nature of the nanotube components in the crosses. © *2000 American Institute of Physics.* [S0003-6951(00)03513-0]

Electrical gates are important elements in semiconductor devices[1] and mesoscopic quantum dots.[2] Gating to nanotube molecular wires has also facilitated the elucidation of electrical properties of various types of nanotubes. For instance, electrons can be added to a metallic single-walled carbon nanotubes (SWNT) segment one at a time at low temperatures by tuning the gate voltage.[3,4] Individual semiconducting SWNTs can turn into electrical ON or OFF states under various gate voltages, exhibiting field-effect transistor characteristics.[5–7] For a large diameter (~3 nm) semiconducting SWNT (S–SWNT) with a primary band gap on the order of 0.2 eV, sufficiently high gate voltages (>40 V) can lead to *n*-type system from *p* type.[8] Recently, small band gap (~10 meV) S–SWNTs are observed, as variations in the gate voltage by several volts causes transitions between *p*-type and *n*-type systems.[9] Also, gate controlled superconductivity proximity effects have been reported in SWNTs contacted by Nb electrodes, suggesting the transparency of metal-tube contacts tunable by gate voltages.[10]

Typically, conducting silicon substrates are used as backgates for SWNT samples obtained on SiO_2/Si substrates. Metal electrodes have also been used as sidegates. The dimension of these gates and the tube-gate distances are macroscopic relative to the size (diameter) of the nanotubes. These gates are coupled to the length of the nanotubes, affecting the potential along the nanotubes uniformly. Herein, we report the utilization of atomic force microscopy (AFM) probe tips to locally gate individual SWNTs. The scanning-probe gates are sharp points (~10 nm in radius) and mobile. The gating probe tips are typically scanned perpendicular to a SWNT, allowing the gate-tip distance adjusted in a range between a few nanometers to microns. Several aspects of the local gating results are found to differ from those of backgating to individual semiconducting and metallic SWNTs. These results shed light into backgating effects to metal-tube contact junctions. Room temperature electrical properties of metal–metal and metal–semiconductor SWNT crosses are also investigated by the current work. Scanning-probe gating proves to be a useful approach to identify the nature of SWNT components in the crosses.

[a)]Electronic mail: hdai@chem.stanford.edu

The SWNT samples were obtained by chemical vapor deposition on SiO_2/Si substrates containing patterned catalyst islands arranged into parallel rows. Detailed SWNT growth and device fabrication were described previously.[7,11,12] The highly doped p^+-Si substrate was used as a backgate, and the thickness of the thermally grown SiO_2 was 500 nm. The metal used to contact SWNTs was 20-nm-thick Ti placed on top of the SWNTs with contact lengths ~1 μm. AFM imaging was carried out to identify electrical circuits formed by individual SWNTs as well as crossing SWNTs grown from adjacent catalyst islands. The spacing between metal electrodes was ~3–5 μm, which sets the typical length of our individual SWNTs. AFM images of representative individual and crossing SWNT devices are shown in Fig. 1.

Figure 1(a) shows the experimental setup for scanning-probe gating of SWNTs. Electrical connections were made to the AFM tip, the silicon backgate and the desired SWNT device after the sample was mounted onto an AFM stage. This allowed for *in situ* AFM operation and electrical measurements. The AFM was operated in the tapping mode to first locate and image the SWNT. In a typical scanning-probe gating experiment, a voltage was applied to the AFM tip while it scanned back and forth across a fixed point of the SWNT over a scan range of 0.3–3 μm. The SWNT was typically at the center of the scan range [Fig. 1(a)]. During

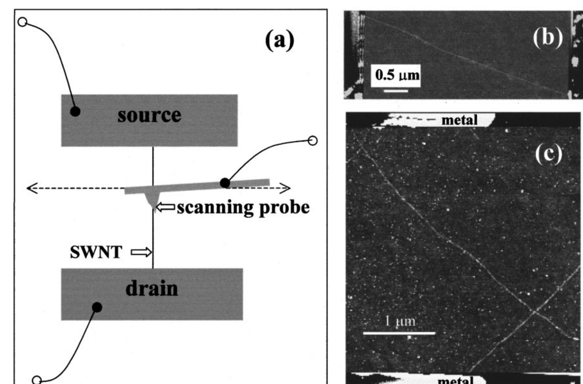

FIG. 1. (a) Schematic experimental setup for scanning-probe gating of SWNTs. (b) AFM image of a representative individual SWNT device. (c) AFM image of a SWNT cross.

 © 2000 American Institute of Physics
Downloaded 22 May 2001 to 128.125.12.30. Redistribution subject to AIP license or copyright, see http://ojps.aip.org/aplo/aplcr.jsp

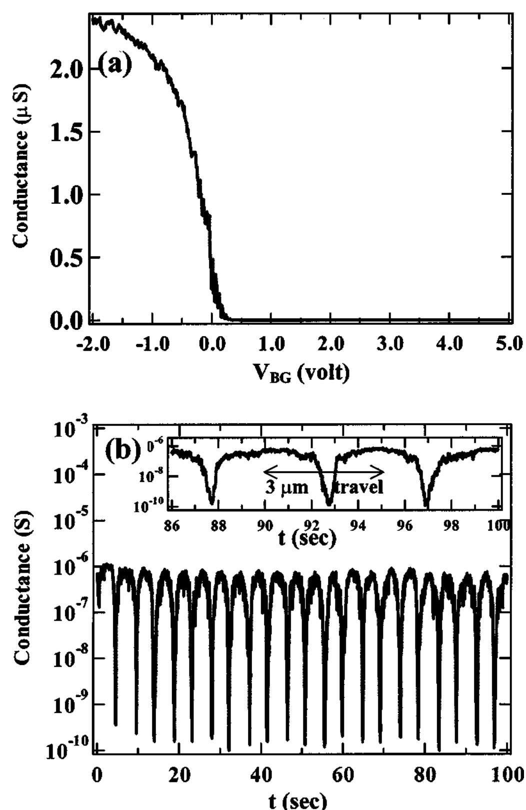

FIG. 2. (a) Conductance vs backgate voltage for a S–SWNT. (b) Conductance vs time under scanning-probe gating voltage for the S–SWNT. Inset: zoomed-in data between $t=86$–100 s.

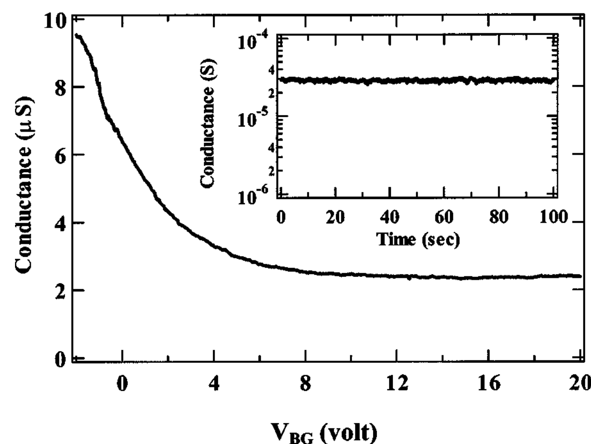

FIG. 3. Conductance vs backgate voltage for a M–SWNT. Inset: Conductance vs time under scanning-probe gating voltage for the M–SWNT.

the repeated scans, the resistance of the SWNT sample was monitored by applying a constant bias voltage across the tube and measuring the current as a function of time. The AFM tip was the closest to the SWNT when the tip tapped on the SWNT, with an averaged tube-tip spacing of ~5 nm due to the tapping actions of the tip. This scanning-probe gating scheme allowed us to investigate how various gate-tube distances affect the electrical properties of SWNTs in real time.

We first present gating results obtained with individual S–SWNTs. Figure 2(a) shows the conductance versus backgate voltage curve for a length ~4 μm, diameter ~1.5 nm semiconducting tube. Under zero backgate voltage ($V_{BG}=0$), a resistance of ~2.4 MΩ was measured for the SWNT. Positive backgate voltages led to four orders of magnitude decrease in conductance while negative backgate voltages enhanced the sample conductance. These characteristics are signatures of *p*-type S–SWNTs.[5–7] Scanning-probe gating was carried out with $V_{TG}=2$ V on the tip scanned over a 3 μm range at a speed of 0.6 μm/s (scan frequency 0.1 Hz). The conductance of the sample was recorded every 10 ms over a time duration of several minutes. As shown in Fig. 2(b), the conductance of the SWNT sample decreased by four orders of magnitude each time the AFM tip scanned over and tapped on the nanotube. The period in the conductance oscillation is 5 s, half of the period of the tip scan. As the tip moved away from the tube, the sample conductance recovered exponentially [Fig. 2(b) inset] with the increase in tip-tube distance. For tip-tube distance >~150 nm, tip gating had little effect on the conductance of the S–SWNT sample. We also applied negative voltages on the tip and found as the sample conductance unchanged as the AFM tip scanned over the SWNT (data not shown). This result differed from that obtained with backgate, as negative backgate voltages enhanced the conductance of the S–SWNT sample shown in Fig. 2(a).

The backgating and scanning-probe gating results shown in Fig. 2 are highly reproducible with different S–SWNT samples. For scanning-probe gating, the results can be rationalized by considering local gating effects. In the case of positive tip-gate voltages, a positive potential is applied to a small segment of the S–SWNT when the tip crosses the tube. The nanotube valence and conduction bands bend downward locally away from the Fermi level, causing local hole depletion in the *p*-type S–SWNT and thus a sharp decrease in the conductance of the nanotube ''channel.'' That is, the local band dip poses a barrier to hole transport, lowering the conductance of the system. In the case of negative tip-gate voltages, upward local band bending should occur but has little effect to the nanotube conductance. This is because the system is dominated by the resistance across the metal-tube junctions, which is unaffected by the AFM tip far away (~1.5–2 μm) from the contacts.

Backgating and scanning-probe gating results obtained with a metallic SWNT (M–SWNT) (length~4 μm, diameter~1.5 nm) are shown in Fig. 3. The room temperature resistance of this sample was ~150 kΩ measured under $V_{BG}=0$. The sample conductance was found to vary with backgate voltage, but showed no depletion under high positive V_{BG}. This backgate dependence, frequently observed with our individual M–SWNTs contacted by Ti, was far from negligible although much weaker than S–SWNT samples. In contrast to the backgating result, Fig. 3 inset shows that scanning-probe gating to the M–SWNT with up to ±10 V on the AFM tip had little effect on the sample resistance. This result suggests that the observed conductance changes of the M–SWNT sample under various backgate voltages should correspond to changes in the metal-tube junctions. The tunable metal-tube contacts by backgate was suggested in a recent study that observed gate-controlled superconducting proximity effect in SWNTs contacted by superconducting Nb electrodes.[10] In this case, only under certain backgate voltages were pronounced proximity effects observable.[10] Since the observation of Andreev reflection requires high transparency between a superconductor and a

Downloaded 22 May 2001 to 128.125.12.30. Redistribution subject to AIP license or copyright, see http://ojps.aip.org/aplo/aplcr.jsp

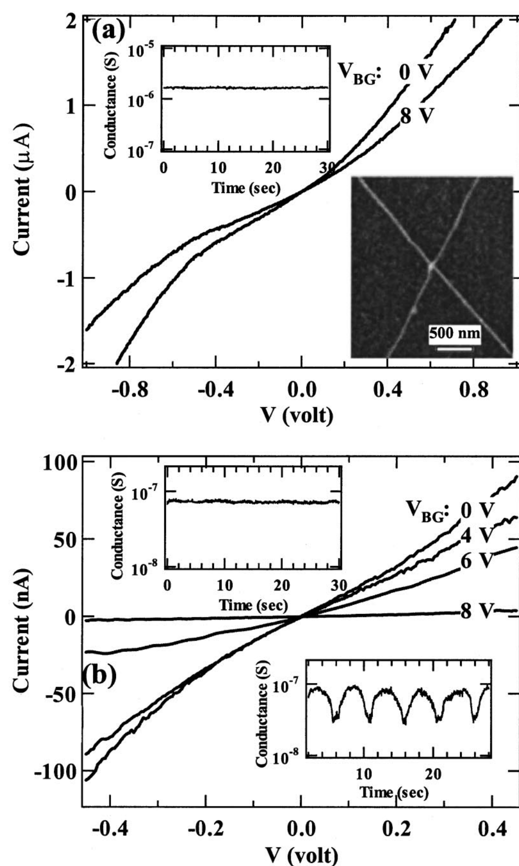

FIG. 4. (a) $I-V$ characteristics of a metal–metal SWNT cross. Left inset: scanning-probe gating results on one of the M–SWNTs. Data (not shown) for the other M–SWNT is similar. Right inset: AFM image of the cross. (b) $I-V$ characteristics of a metal–semiconductor SWNT cross. Right and left insets: scanning-probe gating results on the M–SWNT and S–SWNT, respectively.

normal metal,[13] the backgate controlled proximity effects suggest that the metal-tube contact transparency was enhanced by certain gate voltages.[10] The precise origin of gate controlled metal (e.g., Ti, Nb)-tube contacts remains under investigation. Nevertheless, we observed that the type of contact metal seemed to play an important role. For instance, we found that the conductance of M–SWNTs contacted by Al exhibited little dependence on backgate voltages.[14]

We also investigated the electrical properties of SWNT crosses and employed scanning-probe gating to identify the metallic or semiconducting nature of the SWNT components. Figure 4(a) shows the current–voltage ($I-V$) curves recorded with a SWNT cross (Fig. 4 right inset). The diameters of the SWNTs were 2.7 and 3 nm, respectively. The $I-V$ curve recorded under $V_{BG}=0$ exhibited two linear regions in $|V|<\sim 300$ mV and $|V|>400$ mV, with resistance of ~600 and 400 kΩ, respectively. Scanning-probe gating on each of the two SWNTs found no conductance change of the sample for tip-gate voltages up to 10 V [Fig. 4(a) left inset], suggesting that both SWNTs should be metallic. The typical resistance of individual M–SWNTs in our system ranged from ~15 to ~200 kΩ. The 600 kΩ resistance for the cross should be dominated by the tube–tube contact. The conductance of the metal–metal SWNT cross exhibited weak backgate dependence as shown in Fig. 4(a), and large backgate voltages led to no depletion of the system.

Figure 4(b) shows the $I-V$ curves recorded with a metal–semiconductor SWNT cross. The linear resistance of the cross was ~5.5 MΩ under $V_{BG}=0$, slightly higher than that of a typical individual S–SWNT contacted by Ti (0.3–5 MΩ). Increasing V_{BG} to 8 V depleted the cross sample, leading to diminished conductance. Thus, the metal–semiconductor SWNT cross exhibited field-effect transistor characteristics, similar to individual S–SWNTs. Scanning-probe gating on the metallic tube had no influence on the conductance of the cross [Fig. 4(b) left inset], while gating on the semiconducting tube led to ~5 fold periodic conductance modulations under a tip voltage of 10 V scanned at 0.56 μm/s at a frequency of 0.1 Hz [Fig. 4(b) right inset]. Thus, the scanning-probe gating approach ruled out the possibility of the cross formed by two S–SWNTs. The metal–semiconducting cross consists of Ti/M–SWNT×S–SWNT/Ti. The Ti/M–SWNT part of the system can be considered as a metal-like electrode (M′) contacting the S–SWNT, effectively resulting a M′/S–SWNT/Ti system. Since the cross exhibits similar resistance and $I-V$ characteristics as a typical individual S–SWNT, the coupling between M′ (i.e., M–SWNT) and S–SWNT can be considered as comparable to that between the S–SWNT and Ti metal. This provides a qualitative picture of S–SWNT coupling to a M–SWNT versus to a metal electrode.

In summary, scanning-probe gating studies of individual semiconducting and metallic SWNTs are presented in this letter. The gating approach allows the elucidation of the electrical properties of SWNTs when only part of the nanotubes is gated. The results shed light to the backgating effects on the metal (Ti)-tube contacts. The electrical properties of SWNT crosses are investigated. The scanning-probe gating approach is used to identify the nature of SWNTs in the crosses.

The authors thank Dr. C. Quate for discussions. This work was supported by NSF, DAPRA/ONR, SRC/Motorola, Laboratory for Advanced Materials at Stanford, National Nanofabrication Users Network, the Camile Henry-Dreyfus Foundation, a Stanford Graduate fellowship, and the American Chemical Society.

[1] S. M. Sze, *Physics of Semiconductor Devices* (Wiley, New York, 1981).
[2] M. A. Kastner, Phys. Today **46**, 24 (1993).
[3] S. J. Tans, M. H. Devoret, H. Dai, A. Thess, R. E. Smalley, L. J. Geerligs, and C. Dekker, Nature (London) **386**, 474 (1997).
[4] M. Bockrath, D. H. Cobden, P. L. McEuen, N. G. Chopra, A. Zettl, A. Thess, and R. E. Smalley, Science **275**, 1922 (1997).
[5] S. Tans, A. Verschueren, and C. Dekker, Nature (London) **393**, 49 (1998).
[6] R. Martel, T. Schmidt, H. R. Shea, T. Hertel, and P. Avouris, Appl. Phys. Lett. **73**, 2447 (1998).
[7] H. Soh, C. Quate, A. Morpurgo, C. Marcus, and J. Kong, H. Dai, Appl. Phys. Lett. **75**, 627 (1999).
[8] C. Zhou, J. Kong, and H. Dai, Appl. Phys. Lett. **76**, 1597 (2000).
[9] C. Zhou, J. Kong, and H. Dai (unpublished).
[10] A. Morpurgo, J. Kong, C. Marcus, and H. Dai, Science **286**, 263 (1999).
[11] J. Kong, H. Soh, A. Cassell, C. F. Quate, and H. Dai, Nature (London) **395**, 878 (1998).
[12] J. Kong, C. Zhou, A. Morpurgo, T. Soh, C. Marcus, C. Quate, and H. Dai, Appl. Phys. A: Mater. Sci. Process. **69**, 305 (1999).
[13] G. E. Blonder, M. Tinkham, and T. M. Klapwijk, Phys. Rev. B **25**, 4515 (1982).
[14] J. Kong and H. Dai (unpublished).

Downloaded 22 May 2001 to 128.125.12.30. Redistribution subject to AIP license or copyright, see http://ojps.aip.org/aplo/aplcr.jsp